CLNS 02/1792
CLEO 02-10
CLEO CONF 02-04
ICHEP02-941

Dalitz Analysis of $D^0 \to K^0_S\pi^+\pi^-$

CLEO Collaboration

(July 22, 2002)

Abstract

In e^+e^- collisions using the CLEO detector we have studied the decay of the D^0 to the final state $K^0_S\pi^+\pi^-$ with the initial flavor of the D^0 tagged in charged D^* decay. We use the Dalitz technique to measure the resonant substructure in this final state and clearly observe ten different contributions by fitting for their amplitudes and relative phases. We observe a $K^{*+}\pi^-$ component which arises from doubly Cabibbo suppressed decays or $D^0 - \overline{D^0}$ mixing.

H. Muramatsu,[1] S. J. Richichi,[1] H. Severini,[1] P. Skubic,[1] S.A. Dytman,[2] J.A. Mueller,[2] S. Nam,[2] V. Savinov,[2] S. Chen,[3] J. W. Hinson,[3] J. Lee,[3] D. H. Miller,[3] V. Pavlunin,[3] E. I. Shibata,[3] I. P. J. Shipsey,[3] D. Cronin-Hennessy,[4] A.L. Lyon,[4] C. S. Park,[4] W. Park,[4] E. H. Thorndike,[4] T. E. Coan,[5] Y. S. Gao,[5] F. Liu,[5] Y. Maravin,[5] I. Narsky,[5] R. Stroynowski,[5] M. Artuso,[6] C. Boulahouache,[6] K. Bukin,[6] E. Dambasuren,[6] K. Khroustalev,[6] R. Mountain,[6] R. Nandakumar,[6] T. Skwarnicki,[6] S. Stone,[6] J.C. Wang,[6] A. H. Mahmood,[7] S. E. Csorna,[8] I. Danko,[8] G. Bonvicini,[9] D. Cinabro,[9] M. Dubrovin,[9] S. McGee,[9] A. Bornheim,[10] E. Lipeles,[10] S. P. Pappas,[10] A. Shapiro,[10] W. M. Sun,[10] A. J. Weinstein,[10] D. M. Asner,[11,*] R. Mahapatra,[11] H. N. Nelson,[11] R. A. Briere,[12] G. P. Chen,[12] T. Ferguson,[12] G. Tatishvili,[12] H. Vogel,[12] N. E. Adam,[13] J. P. Alexander,[13] K. Berkelman,[13] F. Blanc,[13] V. Boisvert,[13] D. G. Cassel,[13] P. S. Drell,[13] J. E. Duboscq,[13] K. M. Ecklund,[13] R. Ehrlich,[13] L. Gibbons,[13] B. Gittelman,[13] S. W. Gray,[13] D. L. Hartill,[13] B. K. Heltsley,[13] L. Hsu,[13] C. D. Jones,[13] J. Kandaswamy,[13] D. L. Kreinick,[13] A. Magerkurth,[13] H. Mahlke-Krüger,[13] T. O. Meyer,[13] N. B. Mistry,[13] E. Nordberg,[13] J. R. Patterson,[13] D. Peterson,[13] J. Pivarski,[13] D. Riley,[13] A. J. Sadoff,[13] H. Schwarthoff,[13] M. R. Shepherd,[13] J. G. Thayer,[13] D. Urner,[13] B. Valant-Spaight,[13] G. Viehhauser,[13] A. Warburton,[13] M. Weinberger,[13] S. B. Athar,[14] P. Avery,[14] L. Breva-Newell,[14] V. Potlia,[14] H. Stoeck,[14] J. Yelton,[14] G. Brandenburg,[15] D. Y.-J. Kim,[15] R. Wilson,[15] K. Benslama,[16] B. I. Eisenstein,[16] J. Ernst,[16] G. D. Gollin,[16] R. M. Hans,[16] I. Karliner,[16] N. Lowrey,[16] M. A. Marsh,[16] C. Plager,[16] C. Sedlack,[16] M. Selen,[16] J. J. Thaler,[16] J. Williams,[16] K. W. Edwards,[17] R. Ammar,[18] D. Besson,[18] X. Zhao,[18] S. Anderson,[19] V. V. Frolov,[19] Y. Kubota,[19] S. J. Lee,[19] S. Z. Li,[19] R. Poling,[19] A. Smith,[19] C. J. Stepaniak,[19] J. Urheim,[19] Z. Metreveli,[20] K.K. Seth,[20] A. Tomaradze,[20] P. Zweber,[20] S. Ahmed,[21] M. S. Alam,[21] L. Jian,[21] M. Saleem,[21] F. Wappler,[21] E. Eckhart,[22] K. K. Gan,[22] C. Gwon,[22] T. Hart,[22] K. Honscheid,[22] D. Hufnagel,[22] H. Kagan,[22] R. Kass,[22] T. K. Pedlar,[22] J. B. Thayer,[22] E. von Toerne,[22] T. Wilksen,[22] and M. M. Zoeller[22]

[1]University of Oklahoma, Norman, Oklahoma 73019
[2]University of Pittsburgh, Pittsburgh, Pennsylvania 15260
[3]Purdue University, West Lafayette, Indiana 47907
[4]University of Rochester, Rochester, New York 14627
[5]Southern Methodist University, Dallas, Texas 75275
[6]Syracuse University, Syracuse, New York 13244
[7]University of Texas - Pan American, Edinburg, Texas 78539
[8]Vanderbilt University, Nashville, Tennessee 37235
[9]Wayne State University, Detroit, Michigan 48202
[10]California Institute of Technology, Pasadena, California 91125
[11]University of California, Santa Barbara, California 93106
[12]Carnegie Mellon University, Pittsburgh, Pennsylvania 15213
[13]Cornell University, Ithaca, New York 14853
[14]University of Florida, Gainesville, Florida 32611
[15]Harvard University, Cambridge, Massachusetts 02138

*Permanent address: Lawrence Livermore National Laboratory, Livermore, CA 94550.

[16]University of Illinois, Urbana-Champaign, Illinois 61801
[17]Carleton University, Ottawa, Ontario, Canada K1S 5B6
and the Institute of Particle Physics, Canada M5S 1A7
[18]University of Kansas, Lawrence, Kansas 66045
[19]University of Minnesota, Minneapolis, Minnesota 55455
[20]Northwestern University, Evanston, Illinois 60208
[21]State University of New York at Albany, Albany, New York 12222
[22]Ohio State University, Columbus, Ohio 43210

Weak hadronic decays of charmed mesons are expected to proceed dominantly by resonant two-body decays in several theoretical models [1–5]. A clearer understanding of final state interactions in exclusive weak decays is an important ingredient for our ability to model decay rates as well as for our understanding of interesting phenomena such as mixing [6]. In this context an interesting final state is $D^0 \to \overline{K}^0\pi^+\pi^-$ which can proceed through a number of two-body states. Previous investigations [7–11] of the substructure in this channel were limited by statistics to the Cabibbo favored decays. A key motivation is to observe one or more of the $D^0 \to K^0\pi^+\pi^-$ resonant submodes that proceed via mixing or double Cabibbo suppression, such as $K^{*+}\pi^-$ or $K_0(1430)^+\pi^-$, and to measure their phase relative to the corresponding unsuppressed $\overline{K}^0\pi^+\pi^-$ submodes.

This analysis uses an integrated luminosity of 9.0 fb^{-1} of e^+e^- collisions at $\sqrt{s} \approx 10\,\mathrm{GeV}$ provided by the Cornell Electron Storage Ring (CESR). The data were taken with the CLEO II.V configuration of the CLEO II multipurpose detector [12]. In the upgraded configuration, a silicon vertex detector (SVX) was installed [13] and the drift chamber gas was changed from argon-ethane to helium-propane.

The event selection is similar to that used in our search for D^0-$\overline{D^0}$ mixing via the process $D^0 \to \overline{D^0} \to K^+\pi^-$ [14]. We reconstruct candidates for the decay sequence $D^{*+} \to \pi_s^+ D^0$, $D^0 \to K_S^0\pi^+\pi^-$. Consideration of charge conjugated modes is implied throughout this Letter. The charge of the slow pion (π_s^+ or π_s^-) identifies the charm state at $t = 0$ as either D^0 or $\overline{D^0}$. We require the D^{*+} momentum p_{D^*} to exceed 2.0 GeV/c, and we require the D^0 to produce the final state $K_S^0\pi^+\pi^-$. We reconstruct $K_S^0 \to \pi^+\pi^-$ with the requirement that the daughter pion tracks form a common vertex, in three dimensions, with a confidence level $> 10^{-6}$. Signal candidates pass the vertex requirement with 96% relative efficiency. Throughout this Letter, relative efficiency is defined as the number of events passing all requirements relative to the number of events when only the requirement under study is relaxed.

Our silicon vertex detector provides precise measurement of the charged tracks in three dimensions [15]. We exploit the precision tracking of the SVX by refitting the K_S^0 and $\pi^\pm$ tracks with a requirement that they form a common vertex in three dimensions. We use the trajectory of the $K_S^0\pi^+\pi^-$ system and the position of the CESR luminous region to obtain the D^0 production point. We refit the π_s^+ track with a requirement that the trajectory intersect the D^0 production point. We require that the confidence level of each refit exceed 10^{-4}. The signal candidates pass the D^0 mass and decay vertex requirement with 85% and 91% relative efficiency, respectively.

We reconstruct the energy released in the $D^{*+} \to \pi_s^+ D^0$ decay as $Q \equiv M^* - M - m_\pi$, where M^* is the reconstructed mass of the $\pi_s^+ K_S^0\pi^+\pi^-$ system, M is the reconstructed mass of the $K_S^0\pi^+\pi^-$ system, and m_π is the charged pion mass. The experimental resolution function in Q is non-Gaussian, due to a substantial dependence of the width of the specific (Gaussian) resolution on the particular decay configuration. The addition of the D^0 production point to the π_s^+ trajectory yields the resolution $\sigma_Q = 220 \pm 4$ keV, where σ_Q is the core value from a fit to a bifurcated student's t distribution. We obtain a resolution on M of $\sigma_M = 4.8 \pm 0.1\,\mathrm{MeV}$ and a resolution on $m_{K_S^0}$ of $\sigma_{m_{K_S^0}} = 2.4 \pm 0.1\,\mathrm{MeV}$. These resolutions are better than those of earlier studies [7–11], and permit improved suppression of background processes.

We apply a set of 'prophylactic' requirements to exclude candidates with a poorly determined Q, M, or D^0 flight time, and K_S^0 candidates that are likely to be background.

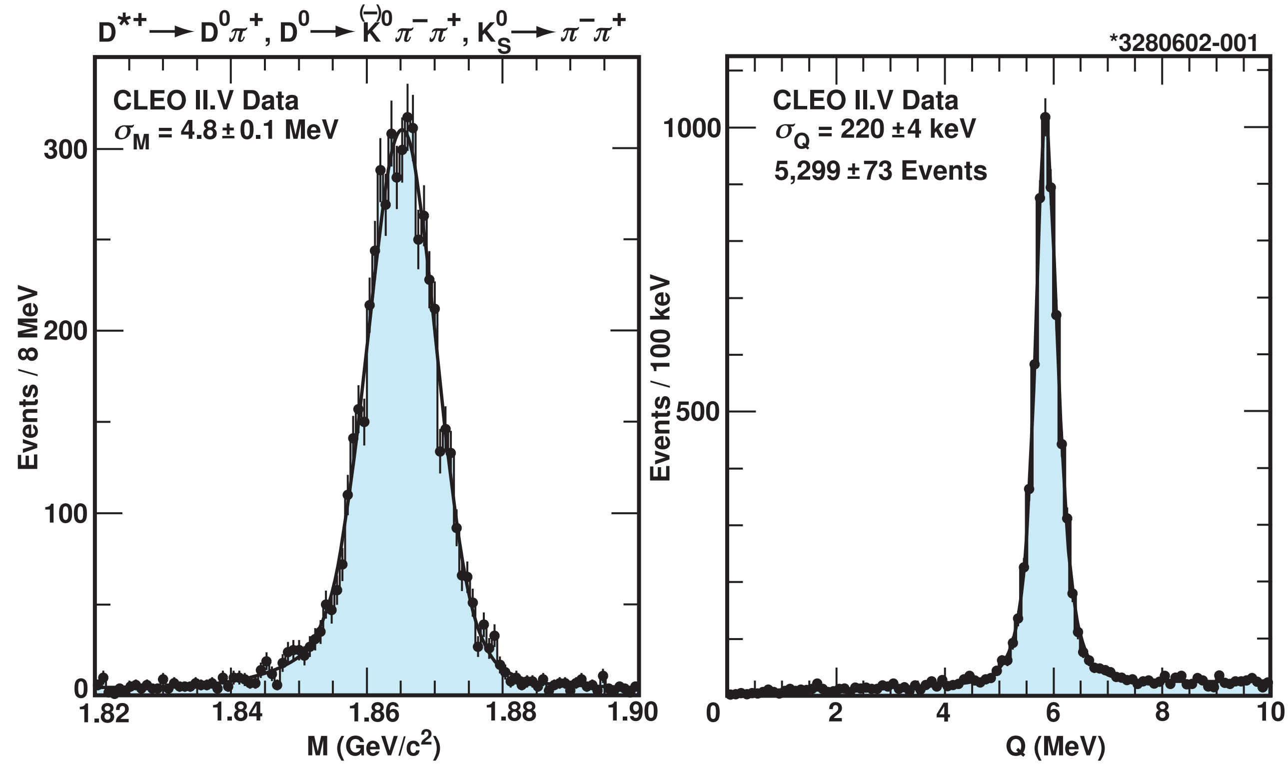

FIG. 1. Distribution of a) Q and b) M for the process $D^0 \to K^0_S\pi^+\pi^-$. The candidates pass all selection criteria discussed in the text.

The typical computed σ for Q, M and flight time error is 150 keV, 5 MeV and 0.5 τ_{D^0}, respectively. These are computed from the reconstruction covariance matrix of the daughters of the D^0 candidate. We require candidates to be well-measured in Q, M and flight time by rejecting those where σ_Q, σ_M or flight time error exceeds 300 keV, 10 MeV or $2.0\tau_{D^0}$, respectively. The relative efficiencies for the signal candidates to pass these cuts is 98%, 98% and 89%, respectively. We exclude K^0_S candidates with a vertical flight distance less then 500 microns to remove combinatoric background with zero lifetime. The signal candidates survive this requirement with 95% relative efficiency. The distributions of Q and M for our data are shown in Figure 1.

We select 5299 candidates within three standard deviations of the expected Q, M, and $m_{K^0_S}$. The efficiency for the selection described above is nearly uniform across the Dalitz distribution. In our simulation we generate the $D^0 \to K^0_S\pi^+\pi^-$ uniformly populating the allowed phase space. We study our efficiency with a GEANT [16] based simulation of $e^+e^- \to c\bar{c}$ events in our detector with a luminosity corresponding to more than three times our data sample. We observe that our selection introduces distortions due to inefficiencies near the edge of phase space, and fit the efficiency to a two dimensional cubic polynomial in $(m^2_{K^0_S\pi^-}, m^2_{\pi^+\pi^-})$ requiring that the efficiency does not change if the π^+ and π^- are interchanged. Our standard result uses this efficiency parameterization to interpret the Dalitz distribution. To take into account a systematic uncertainty in our selection efficiency we compare the standard result with an efficiency that is uniform across the allowed Dalitz distribution.

Figure 1 shows that the background is small, but non-negligible. Fitting the M distribution to a signal shape as described above plus a linear background shape we find a background fraction of $2.1 \pm 1.5\%$. We use this fraction as a constraint when fitting the Dalitz distribution. To model the background contribution in the Dalitz distribution we consider those events in the data that are in sidebands five to ten standard deviations from the signal in Q and M and within three in $m_{K_S^0}$. There are 445 candidates in this selection, about four times the amount of background we estimate from the signal region. We compare these with background from our simulation also including e^+e^- annihilations producing the lighter quarks. We note that the background from the simulation is dominated by random combinations of unrelated tracks, and the shape of the background in the simulation and the sideband data sample agree well. The simulation predicts that the background uniformly populates the allowed phase space, and we model this contribution to the Dalitz distribution by fitting the data sideband sample to a two dimensional cubic polynomial in $(m^2_{K_S^0\pi^-}, m^2_{\pi^+\pi^-})$. All parameters except the constant are consistent with zero. Other possible contributions to the background, resonances combined with random tracks and real D^0 decays combined with random soft pions of the wrong charge, are negligible in the simulation. The latter, called mistags, are especially dangerous to our search for "wrong sign" D^0 decays. Mistags populate the Dalitz distribution in a known way that depends on the shape of signal. When we analyze the Dalitz distribution we allow a mistag fraction with an unconstrained contribution. We have looked for the contribution of an anomalous resonance, such as ρ^0 or K^{*-}, plus random tracks to the background in the data by studying the sidebands in Q, M, and $m_{K_S^0}$, and conclude that any such contributions are negligible.

Figure 2 shows the Dalitz distribution for the $D^0 \to K_S^0\pi^+\pi^-$ candidates. A rich structure is evident. Contributions from $K^{*-}\pi^+$ and $K_S^0\rho^0$ are apparent. Depopulated regions exist suggesting destructive interference between some resonances and the dominant decay modes.

We parameterize the $K_S^0\pi^+\pi^-$ Dalitz distribution following the methodology described in Ref. [17] using the same sign convention used in previous investigations of this decay channel [8,11]. The details of our analysis technique follow closely the method described in Ref. [25] and are summarized briefly here. We consider nineteen resonant subcomponents, $K^{*-}\pi^+$, $\kappa(800)^-\pi^+$, $K^*(1410)^-\pi^+$, $K_0^*(1430)^-\pi^+$, $K_2^*(1430)^-\pi^+$, $K^*(1680)^-\pi^+$, $K_3^*(1780)^-\pi^+$, $K_S^0\rho$, $K_S^0\omega$, $K_S^0\rho(1450)$, $K_S^0\rho(1700)$, $K_S^0\sigma(500)$, $K_S^0f_0(980)$, $K_S^0f_2(1270)$, $K_S^0f_0(1370)$, $K_S^0f_0(1500)$, $K_S^0f_0(1710)$, and the "wrong sign" $K^{*+}\pi^-$ and $K_0^*(1430)^+\pi^-$, as well as a non-resonant contribution. The parameters of the resonances are taken from Ref. [18] except for the f_0's. We use Ref. [19] for the $f_0(980)$ and the coupled channel analysis of Ref. [20] for the $f_0(1370)$, $f_0(1500)$ and $f_0(1710)$. We consider that each of the resonances has its own amplitude and relative phase. The non-resonant contribution is modeled as a uniform distribution across the allowed phase space with a fixed relative phase. The phases and widths of the resonance contributions vary as given by the spin of the resonance as described in Ref. [17].

This method does not strictly conserve unitarity which might lead to an additional systematic uncertainty on the extracted parameters. This is a concern for the scalar mesons which decay to $\pi^+\pi^-$ and contain a number of strongly overlapping resonances. We also do not describe the effect of dynamical threshold openings, which affects resonances close to threshold such as the f_0's.

This study is sensitive only to relative phases and amplitudes (*i.e.* the overall normalization is arbitrary). Thus we fix one phase and one amplitude. To minimize correlated errors on the phases and amplitudes we choose the largest color suppressed mode, $K_S^0\rho$, which should be out of phase with the unsuppressed modes to have a fixed zero phase and an amplitude of one. Since the choice of normalization, phase convention, and amplitude formalism may not always be identical for different experiments, fit fractions are reported in addition to amplitudes to allow for more meaningful comparisons between results. The fit fraction is defined as the integral of a single component divided by the coherent sum of all components. The sum of the fit fractions for all components will in general not be unity because of the effect of interference.

Backgrounds, combinatorics and mistags, are considered as described above. They do not interfere with the signal, but the mistag background shape depends on the signal shape as noted earlier.

One must also consider the statistical errors on the fit fractions. We have chosen to use the full covariance matrix from the fits to determine the errors on fit fractions so that the assigned errors will properly include the correlated components of the errors on the amplitudes and phases. After each fit, the covariance matrix and final parameter values are used to generate 500 sample parameter sets. For each set, the fit fractions are calculated and recorded in histograms. Each histogram is fit with a single Gaussian to extract its width, which is used as a measure of the statistical error on the fit fraction.

We perform an initial fit, using the unbinned maximum likelihood technique including the resonances observed by E687 [11]. We then consider each of the intermediates states listed above retaining those that are more than three standard deviations significant. We do not find the $\kappa(800)^-\pi^+$, $K^*(1410)^-\pi^+$, $K_3^*(1780)^-\pi^+$, $K_S^0\rho(1450)$, $K_S^0\rho(1700)$, $K_S^0 f_0(1500)$, $K_S^0 f_0(1710)$, and the"wrong sign" $K_0^*(1430)^+\pi^-$ to be significant. The $K_S^0\sigma(500)$ is a special case. It is excluded in our standard fit, and its possible contribution is discussed further below. The remaining ten resonances, a non-resonant contribution, and backgrounds as described above are included in our standard fit and give our central results. It has 22 free parameters from ten relative amplitudes and phases describing the signal plus two normalizations for the combinatoric and mistag backgrounds.

Table I gives the results of our standard fit. Figure 2 shows the three projections of the fit. We note that there is a significant "wrong sign" $D^0 \to K^{*+}\pi^-$ amplitude. Mistags are not significant, having a rate of $0.1 \pm 0.4\%$. When we compare the likelihood of our standard fit to one where the $K^{*+}\pi^-$ amplitude fixed to zero we see that the statistical significance of the $K^{*+}\pi^-$ amplitude is 5.5 standard deviations. Also we note that the phase difference between the $K^{*-}\pi^+$ and $K^{*+}\pi^-$ contributions is consistent with 180°, as expected from Cabibbo factors.

We consider systematic uncertainties that arise from our model of the background, the efficiency, and biases due to experimental resolution. Our general procedure is to change some aspect of our standard fit and interpret the change in the values of the amplitudes and phases as an estimate of the systematic uncertainty. The background is modeled with a two dimensional cubic polynomial and the covariance matrix of the polynomial coefficents determined from a sideband. Our standard fit fixes the coefficients of the background polynomial, and to estimate the systematic uncertainty on this background shape we perform a fit with the coefficients allowed to float constrained by the covariance matrix. Similarly we perform a fit with a uniform efficiency rather than the efficiency shape determined from the simulation as an estimate of the systematic uncertainty due to the efficiency. We change selection criteria in the analysis to test whether our simulation properly models the efficiency. We introduce a track momentum cut of 350 MeV/c to avoid the difficulty of modeling our low momentum tracking efficiency, we expanded the signal region from three to six standard deviations in Q, M, and $m_{K^0_S}$, and increased the p_{D^*} cut from 2.0 to 3.0 GeV/c. To study the effect of the finite resolution our experiment has on the variables in the Dalitz plots we vary the size of the bins used to compute the overall normalization.

Another class of systematic uncertainties arise from our choices for the decay model for $D^0 \to K^0_S\pi^+\pi^-$. We consider the Zemach formalism [21], rather than the standard helicity model, which enforces the transversality of intermediate resonances and we vary the radius parameter [22] for the intermediate resonances and for the D^0 between zero and twice their standard value of 0.3 fm and 1 fm, respectively. These variations to the standard fit are the largest contribution to our quoted systematic errors. Additionally, we allow the masses and widths for the intermediate resonances to vary within their known errors [18–20].

We also consider uncertainty arising from which resonances we choose to include in our fit to the Dalitz plot. We compared the result of our standard fit to a series of fits where each of the possible resonances were included one at a time. We also considered a fit including all possible resonances. We take the maximum variation of the amplitudes and phases from the standard result compared to the results in this series of fits as a measure of the uncertainty due to our choice of included resonances.

A few of these additional contributions deserve further discussion. The heavy $\pi\pi$ scalar resonances $f_0(1500)$ and $f_0(1710)$ show large contributions in some of the fits. This is unlikely to be an accurate description of the data as these resonances are relatively narrow, have kinematically excluded central masses, and give a flat and featureless distribution across the Dalitz plot which is difficult to distinguish from non-resonant signal and background. The $\sigma(500)$ has been reported by E791 in $D^+ \to \pi^-\pi^+\pi^+$ decays [23]. The parameters of the $\sigma(500)$ are sensitive to the choice of decay model, discussed previously. Replacing the non-resonant contribution in our standard fit with a $K^0_S\sigma(500)$ component yields an amplitude of 0.57 ± 0.13 and phase of 214 ± 11 with a mass of $m_\sigma = 513 \pm 32$ and width $\Gamma_\sigma = 335 \pm 67$ MeV for the $\sigma(500)$ consistent with E791 results [23] ($m_\sigma = 478 \pm 29$ and $\Gamma_\sigma = 324 \pm 46$ MeV). While we find this suggestive that there is a $K^0_S\sigma(500)$ contribution, we are unable to definitively confirm this because of the known shortcomings of our description of the scalar resonances, as mentioned above. The systematic uncertainty does include the difference between the standard fit which does not include the $\sigma(500)$, and the fits allowing it. On the other hand none of our fits show any evidence for a scalar $\kappa^- \to K^0_S\pi^-$ as also suggested by E791 [24] in charm decays.

We also do separate standard fits for D^0 and $\overline{D^0}$ tags to search for CP violating effects. We see no statistically significant difference between these two fits. A more general study would consider a CP violating amplitude for each component observed in our standard fit.

In conclusion, we have analyzed the resonant substructure of the decay $D^0 \to K^0_S\pi^+\pi^-$ using the Dalitz technique. We observe ten contributions including a "wrong sign" $D^0 \to K^{*+}\pi^-$ amplitude with a significance of 5.5 standard deviations. This decay arises from a double Cabibbo suppressed decay or $D^0 - \overline{D^0}$ mixing. We measure

$$\frac{\mathcal{B}(D^0 \to K^{*+}\pi^-)}{\mathcal{B}(D^0 \to K^{*-}\pi^+)} = (0.5 \pm 0.2^{+0.5}_{-0.1}{}^{+0.4}_{-0.1})\% \ , \quad (1)$$

and the relative phase between the two decays to be

$$(189 \pm 10 \pm 3^{+15}_{-5})^\circ \ , \quad (2)$$

consistent with 180°. We consider D^0 and $\overline{D^0}$ tags separately, and see no CP violating effects.

The time dependence of the Dalitz distribution of this decay mode in our data is able to discern the source of the "wrong sign" signal, doubly Cabibbo suppressed decays or $D^0 - \overline{D^0}$ mixing, and have sensitivity to the mixing parameters x, explicitly to its sign, and y at the few percent level [25].

ACKNOWLEDGMENT

We thank Tim Bergfeld, Pat Burchat, Eugene Golowich, Alexey Petrov and Jon Rosner for valuable discussions. We gratefully acknowledge the effort of the CESR staff in providing us with excellent luminosity and running conditions. This work was supported by the National Science Foundation, the U.S. Department of Energy, the Research Corporation, and the Texas Advanced Research Program.

REFERENCES

[1] M. Bauer *et al.*, Z. Phys. C **34**, 103 (1987).
[2] P. Bedaque *et al.*, Phys. Rev. D **49**, 269 (1994).
[3] L.-L. Chau and H.-Y. Cheng, Phys. Rev. D **36**, 137 (1987).
[4] K. Terasaki, Int. J. Mod. Phys. A **10**, 3207 (1995).
[5] F. Buccella *et al.*, Phys. Lett. B **379**, 249 (1996).
[6] E. Golowich and A. Petrov, Phys.Lett. B **427**, 172-178 (1998).
[7] J. Adler *et al.*, Phys. Lett. B **196**, 107 (1987).
[8] P.L. Frabetti *et al.*, Phys. Lett. B **286**, 195 (1992).
[9] J.C. Anjos *et al.*, Phys. Rev. D **48** 56 (1993).
[10] H. Albecht *et al.*, Phys. Lett. B **308**, 435 (1993).
[11] P.L. Frabetti *et al.*, Phys. Lett. B **331**, 217 (1994).
[12] Y. Kubota *et al.*, Nucl. Instrum. Methods Phys. Res. A **320**, 66 (1992).
[13] T.S. Hill, Nucl. Instrum. Methods Phys. Res. A **418**, 32 (1998).
[14] R. Godang *et al.*, Phys. Rev. Lett. **84**, 5038 (2000).
[15] G. Bonvicini *et al.*, Phys. Rev. Lett. **82**, 4586 (1999).
[16] GEANT manual, CERN Program Library Long Writeup W5013, Copyright CERN, Geneva, 1993.
[17] S. Kopp *et al.*, Phys. Rev. D **63**, 092001 (2001).
[18] D.E. Groom *et al.*, Eur. Phys. J. **C 15**, 1 (2000).
[19] E. M. Aitala *et al.*, Phys. Rev. Lett. **86**, 765 (2001).
[20] A. Kirk, hep-ph/0009168.
[21] C. Zemach, Phys. Rev. B **133**, 1201 (1964).
[22] J. Blatt and v. Weisskopf, *Theoretical Nuclear Physics*, New York: John Wiley & Sons (1952).
[23] E. M. Aitala *et al.*, Phys. Rev. Lett. **86**, 770 (2001).
[24] C. Gobel, hep-ex/0012009.
[25] D. Asner, UCRL-JC-147296-DR.

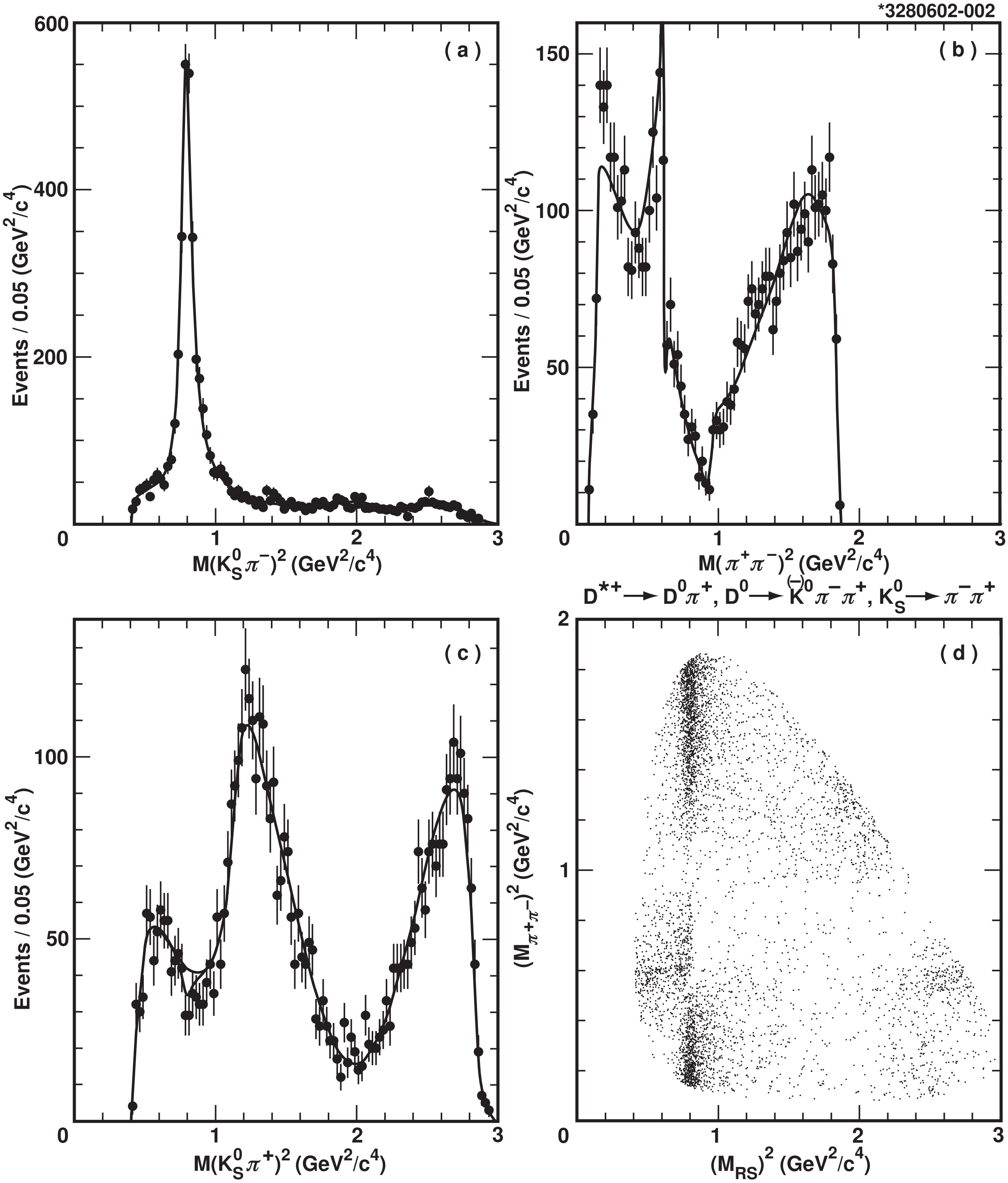

FIG. 2. Projections of the results of the fit described in the text to the $K_S^0\pi^+\pi^-$ Dalitz distribution showing both the fit (histogram) and the data (points). In c) the result of a fit where the "wrong sign" $D^0 \rightarrow K^{*+}\pi^-$ amplitude is fixed to zero is also shown. d) The Dalitz distribution for $D^0 \rightarrow K_S^0\pi^+\pi^-$ candidates. The horizontal axis $(M_{RS})^2$ corresponds to $(M_{K_S^0\pi^-})$ for D^0 and $(M_{K_S^0\pi^+})$ for $\overline{D^0}$.

TABLE I. Standard fit results. The errors shown are statistical, experimental systematic, and modeling systematic respectively. See the text for further discussion.

Component	Amplitude	Phase	Fit Fraction (%)
$K^*(892)^+\pi^-\ \times B(K^*(892)^+ \to K^0\pi^+)$	$(11 \pm 2\ ^{+4}_{-1}\ ^{+4}_{-1}) \times 10^{-2}$	$321 \pm 10 \pm 3\ ^{+15}_{-5}$	$0.34 \pm 0.13\ ^{+0.31}_{-0.03}\ ^{+0.26}_{-0.02}$
$\overline{K}^0\rho^0$	1.0 (fixed)	0 (fixed)	$26.4 \pm 0.9\ ^{+0.9}_{-0.7}\ ^{+0.4}_{-2.5}$
$\overline{K}^0\omega\ \times B(\omega \to \pi^+\pi^-)$	$(37 \pm 5 \pm 1\ ^{+3}_{-8}) \times 10^{-3}$	$114 \pm 7\ ^{+6}_{-4}\ ^{+2}_{-5}$	$0.72 \pm 0.18\ ^{+0.04}_{-0.06}\ ^{+0.10}_{-0.07}$
$K^*(892)^-\pi^+\ \times B(K^*(892)^- \to \overline{K}^0\pi^-)$	$1.56 \pm 0.03 \pm 0.02\ ^{+0.15}_{-0.03}$	$150 \pm 2 \pm 2\ ^{+2}_{-5}$	$65.7 \pm 1.3\ ^{+1.1}_{-2.6}\ ^{+1.4}_{-3.0}$
$\overline{K}^0 f_0(980)\ \times B(f_0(980) \to \pi^+\pi^-)$	$0.34 \pm 0.02\ ^{+0.04}_{-0.03}\ ^{+0.04}_{-0.02}$	$188 \pm 4\ ^{+5}_{-3}\ ^{+8}_{-6}$	$4.3 \pm 0.5\ ^{+1.1}_{-0.4} \pm 0.5$
$\overline{K}^0 f_2(1270)\ \times B(f_2(1270) \to \pi^+\pi^-)$	$0.7 \pm 0.2\ ^{+0.3}_{-0.1} \pm 0.4$	$308 \pm 12\ ^{+15}_{-25}\ ^{+66}_{-6}$	$0.27 \pm 0.15\ ^{+0.24}_{-0.09}\ ^{+0.28}_{-0.14}$
$\overline{K}^0 f_0(1370)\ \times B(f_0(1370) \to \pi^+\pi^-)$	$1.8 \pm 0.1\ ^{+0.2}_{-0.1}\ ^{+0.2}_{-0.6}$	$85 \pm 4\ ^{+4}_{-1}\ ^{+34}_{-13}$	$9.9 \pm 1.1\ ^{+2.4}_{-1.1}\ ^{+1.4}_{-4.3}$
$K_0^*(1430)^-\pi^+\ \times B(K_0^*(1430)^- \to \overline{K}^0\pi^-)$	$2.0 \pm 0.1\ ^{+0.1}_{-0.2}\ ^{+0.5}_{-0.1}$	$3 \pm 4 \pm 4^{+7}_{-15}$	$7.3 \pm 0.7\ ^{+0.4}_{-0.9}\ ^{+3.1}_{-0.7}$
$K_2^*(1430)^-\pi^+\ \times B(K_2^*(1430)^- \to \overline{K}^0\pi^-)$	$1.0 \pm 0.1 \pm 0.1\ ^{+0.3}_{-0.1}$	$155 \pm 7\ ^{+1}_{-4}\ ^{+7}_{-24}$	$1.1 \pm 0.2\ ^{+0.3}_{-0.1}\ ^{+0.6}_{-0.3}$
$K^*(1680)^-\pi^+\ \times B(K^*(1680)^- \to \overline{K}^0\pi^-)$	$5.6 \pm 0.6\ ^{+0.7}_{-0.4} \pm 4.0$	$174 \pm 6\ ^{+10}_{-3}\ ^{+13}_{-19}$	$2.2 \pm 0.4\ ^{+0.5}_{-0.3}\ ^{+1.7}_{-1.5}$
$\overline{K}^0\pi^+\pi^-$ non-resonant	$1.1 \pm 0.3\ ^{+0.5}_{-0.2}\ ^{+0.9}_{-0.7}$	$160 \pm 11\ ^{+30}_{-18}\ ^{+55}_{-52}$	$0.9 \pm 0.4\ ^{+1.0}_{-0.3}\ ^{+1.7}_{-0.2}$